The effect of Radiation on Thermal conductivity of Nano-Structured PANI/Bi$_2$Te$_3$ Composites.

M.S. Shalaby[a],*, N.M. Yousif [a], H.A. Zayed[b], H.M. Hashem[c] , L.A. Wahab[a].

[a] National Center for Radiation Research and Technology, Atomic Energy Authority Nasr City, Cairo, Egypt.

[b] Ain Shams University, Faculty of women for Art Sciences and Education, Heliopois, Cairo.

[c] Physics Department, Faculty of Science, Helwan University, Cairo, Egypt.

Abstract:

Nano-structured Bi$_2$Te$_3$, Polyaniline (PANI) and PANI/ Bi$_2$Te$_3$ were synthesized by Solvothermal method. The crystallite size, Strain, inter-chain separation and unit cell volume were calculated from the X-ray diffraction (XRD) results by using Win fit and Unit cell software. The Gamma irradiation (γ-rays) with dose 50 KGy affects the peaks positions for the PANI samples whereas; it affects the intensity of Bi$_2$Te$_3$ samples. Thermal conductivity measurements were investigated from the differential scanning calorimeter (DSC) with respect to Indium (In) melting temperature curve. 50 KGy dose does not show a remarkable change in the PANI and PANI/ Bi$_2$Te$_3$ values on contrast the value of Bi$_2$Te$_3$ sample was reduced.

Key words: Solvothermal method, XRD, PANI/Bi$_2$Te$_3$, Gamma irradiation, Thermal conductivity

Introduction:

Polyaniline (PANI) is one of most attractive conductive polymers. Due to the easy preparation and low density of PANI, a lot of works have been carried out on PANI and its compositions. The novelty in properties, characterization, and applications was mentioned in many studies [**S. Bhadra et al. (2008**)]. PANI is a semi-crystalline polymer with rarely detailed crystal structure studies [**J.P. Pouget et al. (1991)**]. X-ray diffraction (XRD) is expected to be the most essential method for investigating the structure of a crystalline material. PANI's transport properties affected very well with the type and the number of doping materials [**A. Shakouri et al .(1999), J. Tsukamoto et al. (1990), Y. Hiroshige et al. (2006),H. Yan et al. (1999), Mateeva et al.(1998)**]. An extensive amount of research is being carried out to synthesize and characterize potential thermoelectric (TE) materials for applications in the area of micro-coolers, infrared detectors, and power generation systems [**G. Min et al. (1999), I. Stark et al. (1999), T.M. Tritt et al. (1999)**].

*Corresponding Author: phymshalaby@gmail.com –Moustafa.shalaby@eaea.org.eg

The development of advanced electronic devices has been contributed greatly to thermoelectric technology [**T.M. Tritt et al. (2008), G.J. Snyder et al. (2008)**]. One of the PANI's unique features is the thermoelectric behavior. They possess a high electrical to thermal conductivity ratio when compared to inorganic materials.

A lot of researchers have attempted to synthesize and characterize composites of Bi_2Te_3/PANI [**K. Chatterjee et al.(2009), N. Toshima et al. (2011),X. Xu et al. (2005)**]. Li and his co-workers succeeded in using mechanical blending method for synthesis Bi_2Te_3–PANI; they found that the power factor of the composite is less than both of the individual compartments [**M. Pujula et al. (2016**)]. However, the synthesis of a Bi_2Te_3 and PANI hybrid by physical was mixing and solution mixing. Toshima et al. showed a higher power factor in the case of the physical mixture [**N. Toshima et al. (2011)**]. Structural and Electrical properties of PANI and Bi_2Te_3 have been studied by a lot of researchers [**S. Bhadra et al. (2008)**, **J.P. Pouget et al. (1991), N.S. Abishek et al. (2018), H. Mamur et al. (2018)**]. Thermal conductivity is a very vital tool in investigating thermal properties of such kind of materials with a thermoelectric behavior background. DSC was used by [**M. Pujula et al. (2016**), **D. Sa˙nchez et al. (2015), Camirand et al. (2004), Flynn et al. (1988)**] to calculate the thermal conductivity of polymers and another kind of materials. [**M. Pujula et al., (2016**)] found there is nearly 20-30 % deviation of thermal conductivity of the powder between the experimental and theoretical ones. All of the researchers used the (In) melting peak which achieved from DSC to calculate the thermal conductivity of the samples from the differences in the slopes of the onset (In) melting peak with/without the sample. [**J. H. Flynn et al. (1988**)] method used to evaluate the thermal conductivity for flat and square sheets in shape for both reference and samples. The differences between their methods come back to the shape and the method of calculations to get the final values of the thermal conductivity. Here in the present work, the prepared samples were irradiated with 50 KGy radiation dose. The structure and thermal properties have been investigated before and after the irradiation process.

2. Experimental techniques

2.1 *Synthesis of Bi_2Te_3*

In a beaker of 100 ml capacity, 0.01 mol of Bismuth chloride ($BiCl_3$), 0.15 mol of Tellurium, 0.08 mol of Potassium hydroxide (KOH) and 0.03 mol of Sodium borohydride ($NaBH_4$) were mixed together. Up to 90 ml, the beaker was filled with N-N dimethylformamide (DMF). Then the mixture was kept in a muffle furnace at 100-180°C for 24 hours. After that, the mixture was slowly cooled to the room temperature. The final product was filtered, washed with double distilled water and dried in a vacuum oven at 80°C for 12 hours.

2.2 *Synthesis of PANI and PANI/ Bi_2Te_3 Composite*

A chemical oxidative method was used to prepare PANI [**G. Louran et al.(1996**)]. 0.2 mol Aniline with 0.25 mol Ammonium per sulphate was oxidized in an acidic aqueous medium. Aniline and Ammonium per sulphate were dissolved, separately, in 50 ml solution of 1.0 mol HCl in double distilled water. Both the solutions were kept at room temperature for 1h and were mixed together in a beaker. During the process, the color of the solution changed from colorless to light blue and then to dark green. The solution was briefly stirred and was left to polymerize for 24 h. The precipitate of PANI was collected on a filter paper, washed with distilled water, then with 20 ml of 0.1M HCl and with Methanol. PANI (Emeraldine salt) powder was dried in a vacuum oven at 80°C. A similar procedure was followed for the synthesis of Bi_2Te_3-PANI composite, but this time Bi_2Te_3 was introduced in aniline solution.

2.3 Gamma Radiation Source

^{60}Co Irradiation facility was used to irradiate the samples with dose rate 2.54Gy/Sec. This Facility was constructed by the National Center for Research and Radiation Technology (NCRRT) in Atomic Energy Authority in Egypt.

3. Characterization

3.1 Structural characterization

A fully computerized X-ray diffractometer, Shimadzu XRD-6000, with Cu K$_\alpha$ radiation has a wavelength λ=1.54 Å was used for Phase identification and microstructure analysis as in [**E.Ashalley et al. (2015**)]. The X-ray tube was operated at 40 kV and 30 mA anode current throughout the measurements. The pattern was recorded at a scanning rate of 8˚/ min. To confirm the chemical structures of the Samples with/without 50 Gamma irradiation dose, Raman spectrometer Labram HR Evolution was used, with Argon ion laser at 514 nm at room temperature.

3.1.1 Analysis of X-ray diffraction data

The winfit program was used to make a convolution of the samples. Also, it was used in crystallites size and strain calculations. Unit cell parameters for the samples can be detected from the Unit Cell Program.
The inter-chain separation length (R) corresponding to the most intense crystalline peak was determined from the relation given by Klug and Alexander [**Z.H. Zheng et al. (2012**)].

$$R = \frac{5\lambda}{8\,sin\theta} \qquad (1)$$

3.1.2 Computing and Programming
3.1.2.1 Raman fitting Data

PeakFit is an automated nonlinear peak separation and analysis software package for scientists performing spectroscopy, chromatography and electrophoresis. It automatically finds and fits up to 100 peaks to a data set, at a time, enabling users to characterize peaks and find the best equation that fits their data. PeakFit can also enhance the data obtained from traditional numerical methods and lab instruments.

3.3 Thermal Conductivity measurement

3.3.1 Theoretical backgrounds

A lot of scientific works handle with the thermal conductivity (K) investigations from differential scanning calorimetry (DSC) [**D. Sa˙nchez et al. (2015), C.P. Camirand et al. (2004), J.H. Flynn et al. (1988)]**]. Flynn [**J.H. Flynn et al. (1988)**] found that the rate of heating (β) plays an important role in the calculation of the slopes of the reference metal (In) and powder plus In. Recently, From Miquel Pujula et al., calculations [**J.P. Pujula et al. (2016)**], The equations were used to calculate the thermal conductivity showed that (β) was eliminated that proved that (K) is independent on β. Also, the thermal conductivity was calculated by the method mentioned in [**D. Sa˙nchez et al. (2015), C.P. Camirand et al. (2004), J.H. Flynn et al. (1988)**].
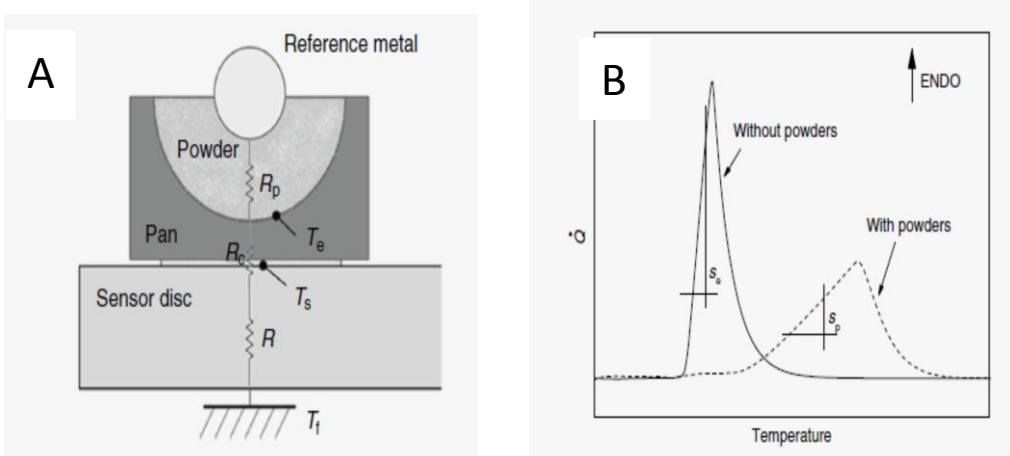

Figure (1): **A)** Geometric appearance of the hemispherical pan placed on the DSC sensor disk. The thermal resistance of the system is indicated (R: sensor, Rc: contact resistance, Rp: powder) **B)** The Slopes of the melting peak of reference metal with and without the powder. [Graph is taken from ref., [**J.H. Flynn et al. (1988)**]]

For powder samples the thermal conductivity calculations use the base of spherical heat conduction transfer and calculated simply from Miquel Pujula et al., method [**M. Pujula et al. (2016)**] by using the relation;

$$\mathrm{K} = \frac{1}{2\pi R_p} \cdot \left(\frac{1}{r_i} - \frac{1}{r_e}\right) \qquad (2)$$

Where r_i and r_e are the radii of the reference and the pan respectively. R_p is the thermal resistance of the investigated sample used in contact with reference as shown in figure (1.A) that simply calculated from :

$$R_p = (\frac{1}{S_p} - \frac{1}{S_e}) \qquad\qquad (3)$$

S_e and S_p are the slopes of the onset low-temperature side of the melting peak of a pure metal (In) without/with the sample's powder respectively, as depicted in figure (1.B).

Here the samples were taken flat and homogeneous after pressed into cylindrical shape fitted with the pan. According to equations in [**M. Pujula et al. (2016)**], β is ignored in calculations by this method because (K) depends only on the density of the samples (ρ), the specific heat (c) and (k) the thermal diffusivity of the material.

3.3.2 Development of the Technique

Thermal conductivity measurements were performed by Shimadzu thermal analysis of type (DSC-50) in Ni flow gas with rate 30 ℃/min. The temperature range was taken from 30-250 ℃ to determine the melting point of the reference metal; (In) with/without the powders under investigations.
The aluminum sample pan came in contact with the sensor disc of DSC, the heat path was considerably altered, and the steady state slope of the melting peak may be affected. So some precautions must take into considerations like the heat flow from the heater of the DSC to the reference metal (In) must pass through the arrangements as in Fig. (1.A), 1) Between the sensor disk and the Pan, 2) Between the Aluminum Pan and the Specimen, 3) Between the Specimen and the reference metal. However, the melting point of the reference metal may vary from specimen to specimen and will vary considerably from one sensor to another. For Ideal investigations, the thermal resistances of (1, 2) should be kept at constant and small as possible with respect to the thermal resistance of the specimen of interest. The reference metal (In) was flattened on the bottom of the pan in order to optimize the thermal contact between the metal and the pan in order to calculate the slope of the melting peak of the reference without the powder (S_e) as depicted in figure (1.A&B). Similarly to the previous technique but the slope of the melting peak of the specimen and the (In), (S_p) could be calculated a corroding to the relations used in [**D. Sa'nchez et al. (2015**)] as depicted in Fig. (1.B). Then R_p and K could be calculated using equs.1 &2 for the powder specimens. The reference metal (In) was contacted with a small area of the sample.

Results and Discussions:
4.1 Structure characterizations:
4.1.1 X-ray diffraction (XRD)

It is well known that polymers have two-phase systems: i) the crystalline phase in which the polymer chains are parallel and ordered in a close-packed array. ii) The semi-crystalline phase where the chains are not ordered and do not have a parallel alignment that is the amorphous region.

The nature of polymer chains in the crystalline/Semi-crystalline phases can be detected from X-ray diffraction study. The diffractogrames of Polyaniline (PANI), PANI/Bi_2Te_3 and Bi_2Te_3 were depicted in Fig. (2). The XRD patterns for PANI are similar to the previously reported data [**A. Shakouri et al.(1999)**] with the same $2\theta°$ and hkl. Three sharp peaks are observed for PANI and PANI/Bi_2Te_3 (Fig. 2) at different angles of diffraction corresponding to 100, 110 and 010 crystal planes, indicating that the majority of PANI chains are ordered on these three crystal planes. The sharpness (width) of the peaks represents the degree of orientation of the polymer chains in that particular crystal plane, and the intensity (peak height) represents the population of crystallites in that plane. It is found that for PANI the sharpness of the 110 crystal plane is the maximum with higher intensity. There is a slight decrease in the full width at half maximum (FWHM) at $20°$ and $25°$ for PANI/Bi_2Te_3 with respect to the pure PANI indicates that the ordering is greater in the parallel direction than in the direction perpendicular to the elongated nano-particle axis. This suggests that Bi_2Te_3 nanoparticles might generate a more ordered molecular alignment of PANI. Bi_2Te_3 peaks are not detected in PANI/Bi_2Te_3 samples that confirm the full interaction of Bi_2Te_3 into backbone chains of PANI. It should be noted that the 50KGy hasn't any remarkable sign on the shape of the PANI peaks but there a slight change in the height of the peaks (intensity) and positions.
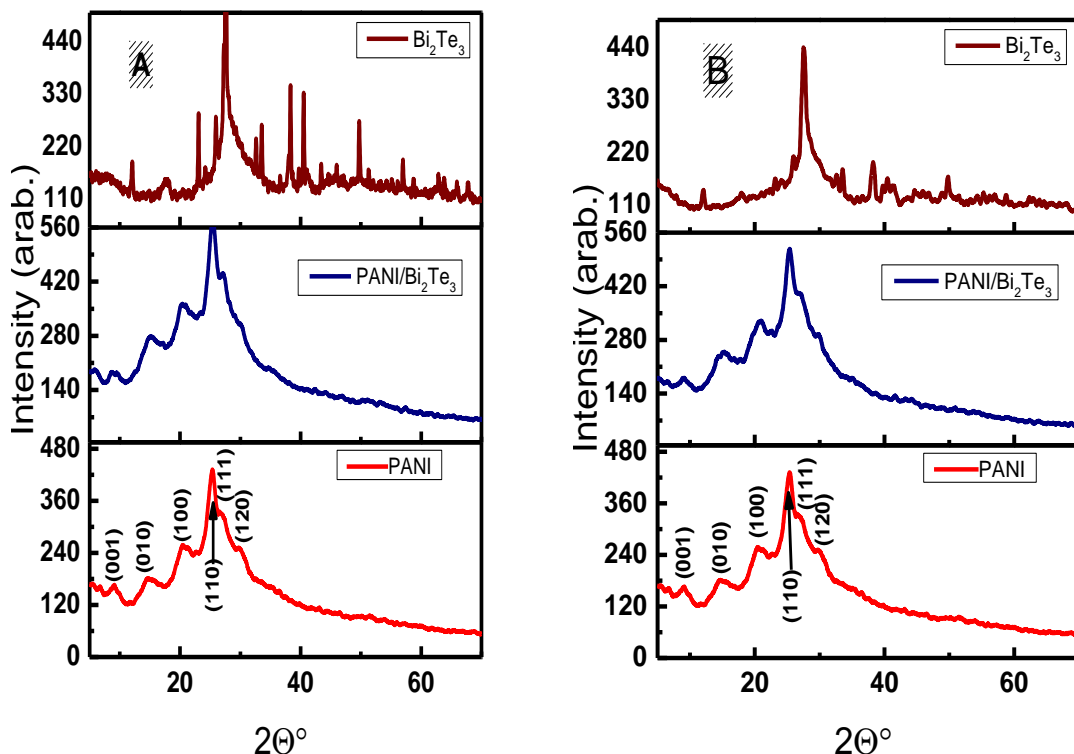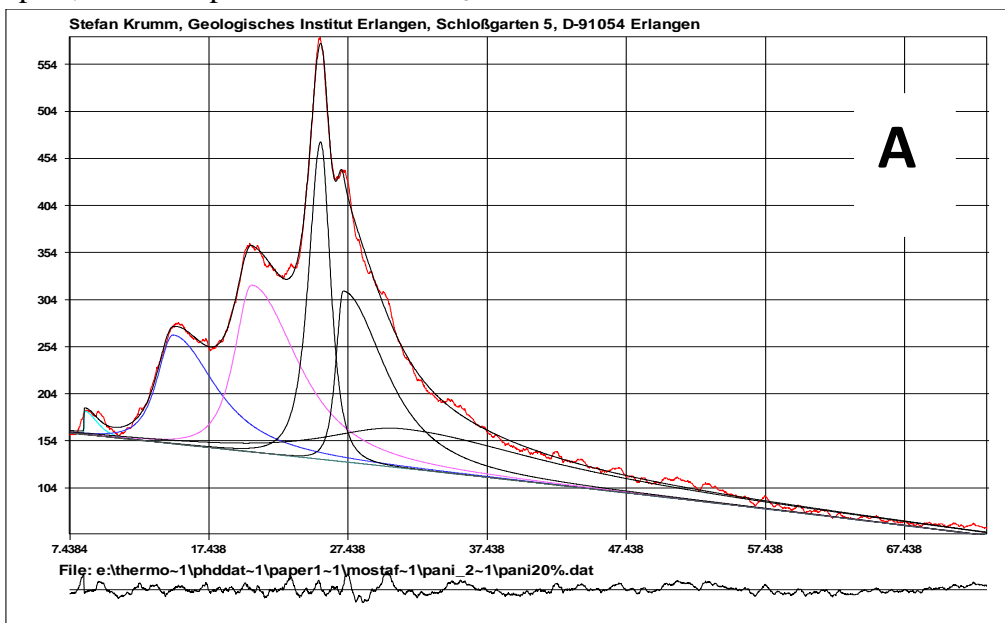
Figure (2): XRD diffractogrames for PANI, PANI/Bi$_2$Te$_3$ and Bi$_2$Te$_3$ samples, **A)** Before Irradiation process, **B)** After Irradiation Process for 50 KGy.

The profile fitting using Winfit program and the representative plots was illustrated in Fig. (3).The grain size and the strain were calculated from Winfit program with respect to the reference of the X-ray instrument that is revealed in Table 1.

The calculated values of crystallite size, strain and inter-chain separation corresponding to the highest intense crystalline peak for the samples are presented in Table 1. The grain size for PANI and PANI/Bi$_2$Te$_3$ increased after irradiation with 50 KGy. In contrast, the strain affected slightly by the irradiation. The inter-chain separations (R) for PANI does not change before/after the 50KGy irradiation but in case of PANI/Bi$_2$Te$_3$ there is a very little change on its value which indicates that the polymer chains in a PANI/Bi$_2$Te$_3$ with 50 KGy crystals are the closest and compact, least compact in PANI/Bi$_2$Te$_3$ without irradiation.
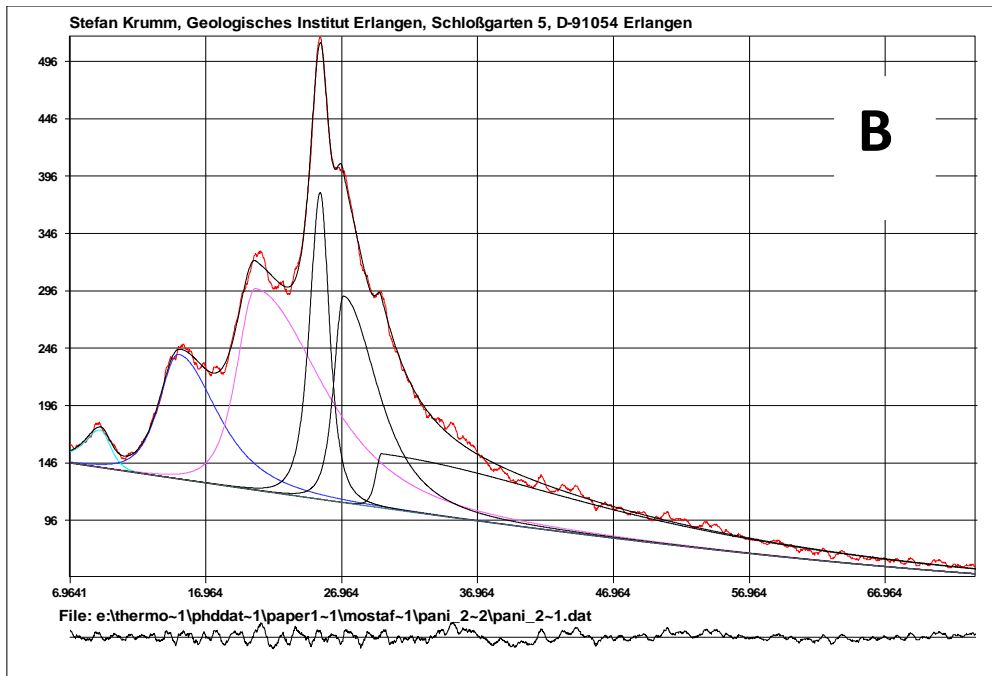
Figure 3: The deconvolution analysis using Winfit program for PANI/Bi$_2$Te$_3$: **A**) 0 KGy, **B**) 50 KGy

According to J. P. Pouget et al., the crystal structures of PANI and PANI/ Bi$_2$Te$_3$ were equivalent in an orthorhombic symmetry, but not in a triclinic one. Unit cell program was used in lattice parameters and unit cell volume calculations. But the unit cell volume for PANI and PANI/ Bi$_2$Te$_3$ was lesser than the unit volume mentioned in [**S. Bhadra et al. (2008), J. Pouget et al. (1999), A. Shakouri et al. (1999)**] and that might be due to: i) the value of the polymer parameter (c) varies of a given corresponds to a zigzag repeat unit containing two rings. ii) The angular distortion along the chain of PANI due to the lesser degree of interchain hydrogen bonding and relatively higher intra-chain H-bonding between the polymer chains.

Figure (2) shows also the diffraction pattern for pure Bi$_2$Te$_3$ before and after the 50KGy irradiation process. The samples are an almost single phase matched with (JCPDC no. 45-0863) with a very little unidentified peak with less than 5%. However, the intensity of the peaks was minimized strongly after the irradiation process whereas the broadening of Bi$_2$Te$_3$ irradiated sample peaks increased that may be caused by: i) the change in atomic percent of the bismuth to the tellurium ii) The irradiation process may Reduce conglomerate of crystallites that confirmed by grain size calculations in Table 1.
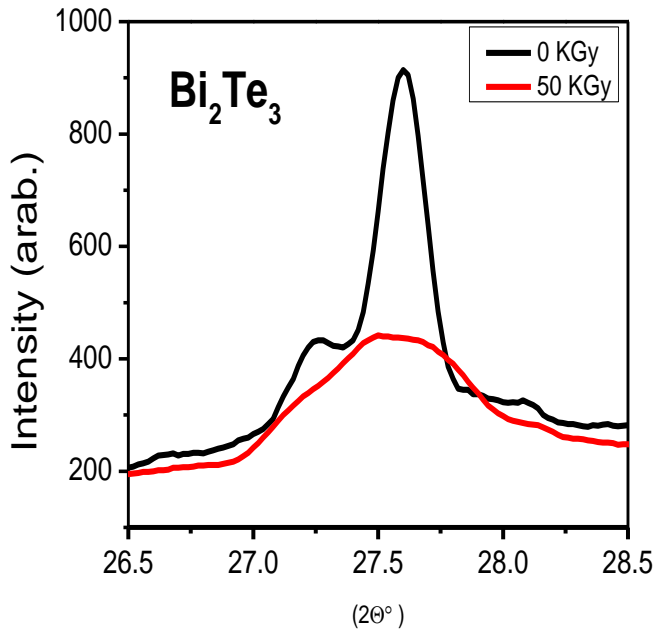
Figure (4): XRD pattern of the most predominant peak of Bi_2Te_3: shows decrease in intensities and a little shift in XRD peak towards the low 2θ˚.

Figure (4) shows how the irradiation process by gamma radiation affects the structure of Bi_2Te_3 by reducing the predominant peak's height and increasing its FWHM which matched with ref. [**J. Tsukamoto et al. (1990)**]. All of those proceedings will reflect on the grain size and the strain calculations as scheduled in Table 1. The determined grain size of Bi_2Te_3 agreed with that published in ref. [**Y. Hiroshige et al. (2006)**].

Table 1: The Grain size, Strain and inter-chain separation (R) corresponding to the highest intense crystalline peak and Unit cell volume of PANI, PANI/ Bi_2Te_3, and Bi_2Te_3

Sample	0 KGy				50 KGy			
	Grain Size (Å)	Strain x10^{-3}	R (Å)	**Unit cell Volume (Å)^3**	Grain Size (Å)	Strain x10^{-3}	R (Å)	**Unit cell Volume (Å)^3**
PANI	36	27	4.39	240.30	49	25	4.39	237.37
PANI/ Bi_2Te_3	40	29	4.40	242.05	44	27	4.38	224.27
Bi_2Te_3	273	--	--	508.84	115	116	--	509.34

4.1.2. **Raman Spectroscopy**

Raman spectroscopy used in the microscope mode is very efficient for the characterization of interactions between the components in conductive polymers composites and blends [**M. Cochet et al. (2000)**]**.** Raman spectra using laser line at 632.8 nm exciting radiation was recorded. Raman Spectra for the samples with/without the 50 KGy Gamma dose are shown in figures (5 A & B).

It is possible to observe intense and broad overlapping bands at 1,312, 1,331 and 1,392 cm^{-1}, corresponding to C–N$^+$, stretching modes of delocalized polaronic charge carriers, which is characteristic of the protonated imines form of Polyaniline. The band at 1,331 cm^{-1} is shifted to 1,365 cm^{-1} with 50 KGy irradiated dose and the band at 1,312 cm^{-1} is shifted to 1,307 cm^{-1} as depicted in ((Appendix I) figures (6 &7)).[**M. Cochet et al. (2000)**, **L. Wang et al. (2015)**]**.** Moreover two important absorptions can be highlighted for PANI with and without irradiation dose: at 669 cm^{-1} and 677 cm^{-1}, related to benzene ring deformation [**M. Cochet et al. (2000)**] and at 429 cm^{-1} and 415 cm^{-1}, assigned to cross linking between PANI chains respectively [**M. Tagowska et al. (2004)**] .The band at 667cm^{-1} has been attributed to the deformation of the benzene ring in the PANI backbone, and according to the literature [**G. Louarn et al. (1996)**].
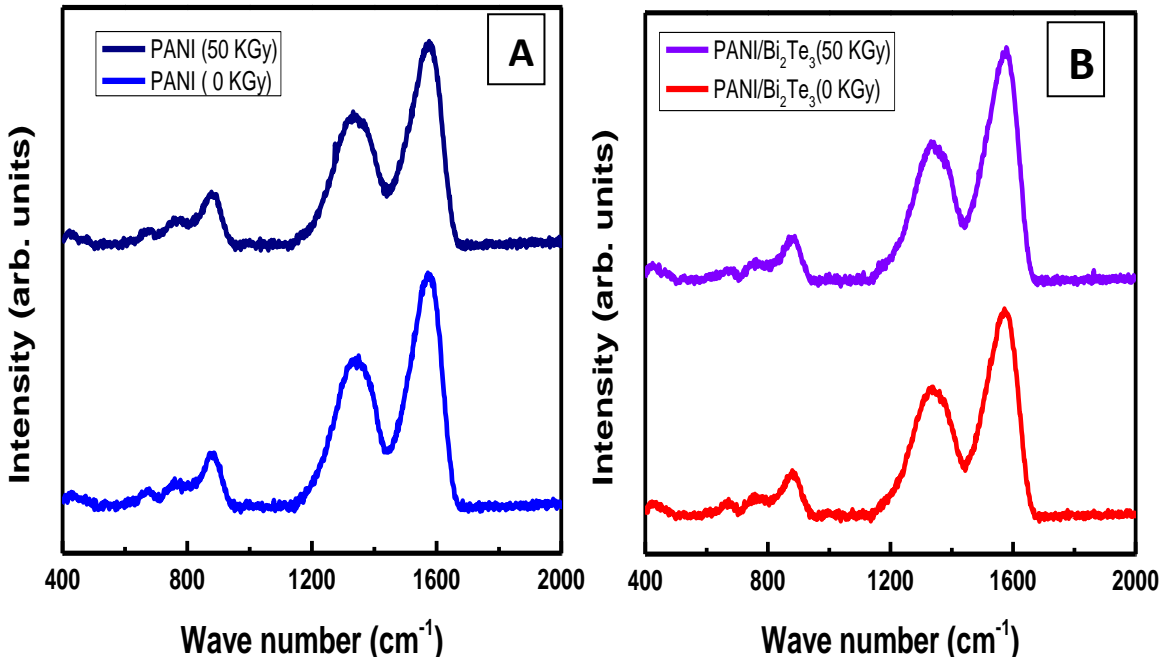
Figure (5): Raman spectrograph recorded for PANI and PANI/Bi_2Te_3samples with/without irradiation 50KGy dose.

On the other hand there are bands 1544 cm^{-1} (C=N stretching of the quinoid rings), 1590 cm^{-1} (C–C stretching of the benzenoid rings), 1392 cm^{-1} and 1590 cm^{-1} (the vibration of delocalized polarons in the extended polymeric conformation) where they appear in the all PANI samples before and after the irradiation process [**L. Wang et al. (2015)].**] as depicted in the convolution figures (1: 3) in Appendix (I). Compared with the pure PANI, the peaks at≈ 1331 cm^{-1} and 1598 cm^{-1} in both PANI and PANI/Bi_2Te_3 composites after the irradiation process obviously shifted to the low frequency, suggesting that there existed strong **π–π** conjugated interactions between Bi_2Te_3 and the polymer because the strong **π–π** conjugated interactions could enhance the electron delocalization and cause a Raman shift.

The conductive nature of PANI can be associated to the band located at 890 cm^{-1} in our case was observed at around 882 cm^{-1} , assigned to deformation C-N of secondary amine next to aromatic ring in the polaronic form C-N$^+$-C [**M.A. Carvalho et al. (2017)**].

In Figure 6, it is appearing that the difference in the intensity between the peaks of Bi_2Te_3 without radiation and with irradiated 50 KGy which confirmed the nano-structured composition of Bi_2T_3. It should be noted that Raman spectroscopy analysis confirmed XRD data. Also, the 50 KGy dose from Gamma rays was affect on the structure of Bi_2Te_3.
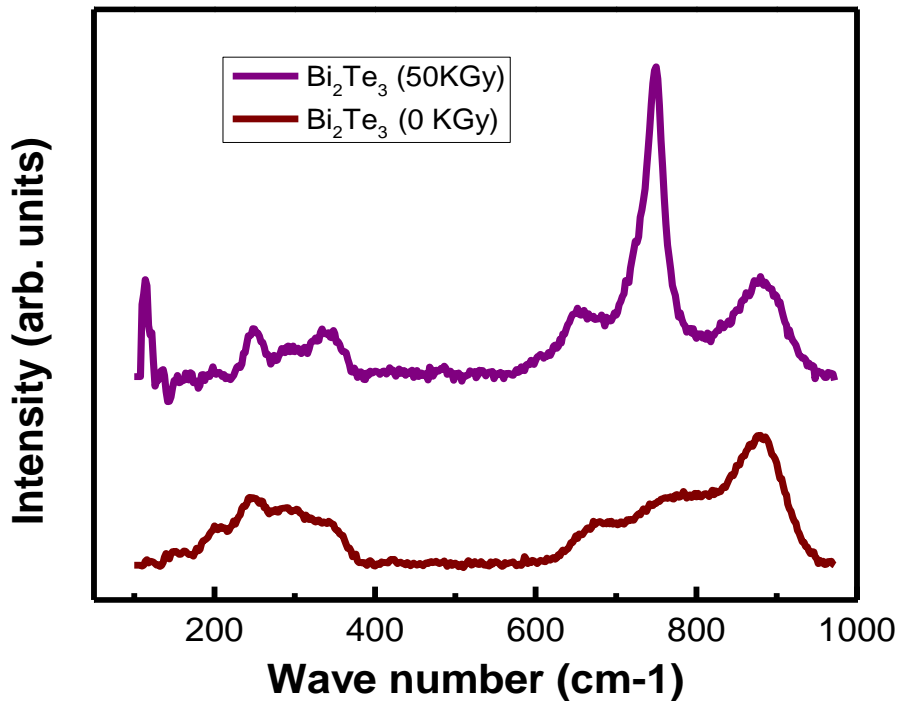
Figure (6): Raman spectrograph recorded for Bi_2Te_3samples with/without irradiation 50KGy dose.

A remarkable peak was observed at 118 cm^{-1} that may the indication of the nanostructured Bi_2Te_3. Specially that, this mode (X peak) was observed in nano-crystalline and few-quintuple thick Bi_2Te_3, and identified as a A^1_u mode as mentioned before in [**Z.H. Zheng et al. (2012), H. Xu et al. (2015), N.S. Abishek et al. (2018), G.D. Keskar et al. (2013)**]. The presence of Te1 atoms in the center of unit cell demands the IR active modes (A^1_u) to be odd parity. Because the polarizability does not change for odd parity modes, in centro-symmetric molecules, they are often Raman inactive [**G. D. Keskar et al. (2013)**]. There two peaks at 250cm^{-1}, 349 cm^{-1} and 652 cm^{-1}, respectively. Their intensity is remarkable especially in the irradiated Bi_2T_3 which may be appeared due to the effect of radiation on the Bi_2Te_3 powder. The radiation dose may break some chemical bonds that affect very well on the Bi: Te ratio also on their modes of vibrations. On the other hand there is a Raman shift at 758cm^{-1} peak to 747 cm^{-1} in the irradiated Bi_2Te_3 sample which is an overtone of the A^2_{1g} mode [**V.Russo et al.(2008)**]

4.2 Thermal Conductivity measurements

The thermal conductivity of the samples powders was measured in N_2 at the melting point of In (156.6℃) with β=10℃/min. The results were mentioned in Table 2.

Due to the powder nature of the samples, the thermal conductivities of them were lower than the reports before with nearly 20% at the same temperature which represents the (In) melting temperature.

And this was expected from earlier researchers before as mentioned in [**D. Sa'nchez et al. (2015**)]. Also, powder behavior is dependent on both the particle shapes and external variables, which is complex and why we cannot accurately predict powder performance from measurements of physical properties alone. Moreover, it is reasonable to say that we do not yet fully understand all of the possible interactions, nor do we have the capability to directly measure many of the influencing parameters.

There is no doubt about the effect of the surrounding gas (N_2) that was used here with 20 ml/min as a flow rate. It may enhance the connectivity between the solid particles to reduce the thermal resistance to transfer more heat through the sample.

Figure (7) show that there are significant differences in the melting temperature of the (In) metal when the reference metal is melted with and without powders contained in the crucible. The relationship between this delay and the thermal conductivity of the powders may be due to the different properties of the powders and the specific heats of the samples.

Table 2: Thermal conductivity dependence parameters for powder Samples.

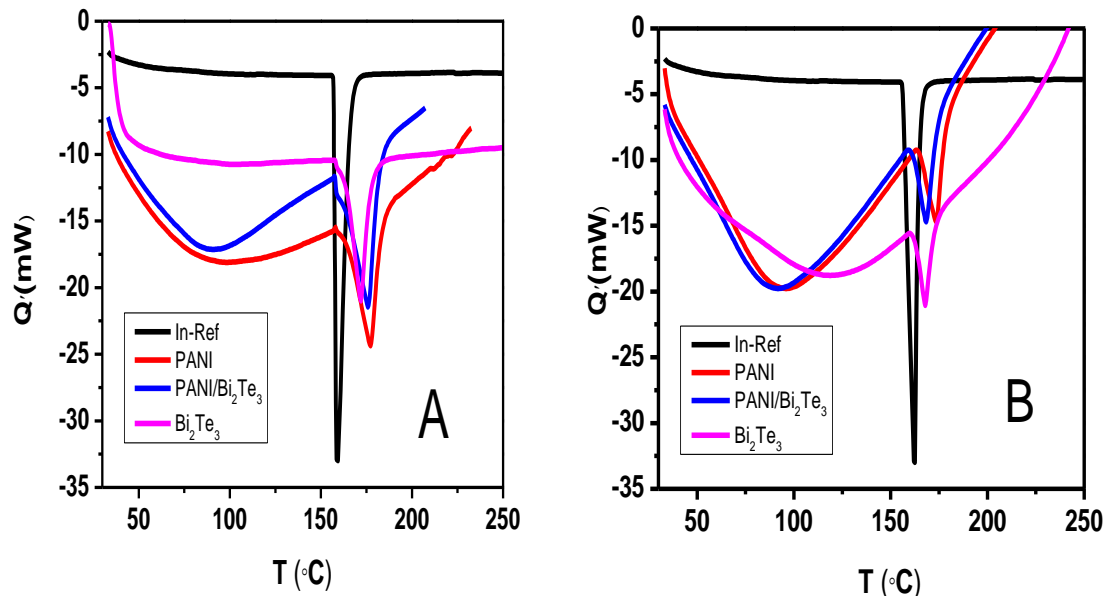| Sample	0 KGy			50 KGy			Thermal conductivity (Ref.)
	Metal Sphere radius (mm)	**Melting Slope (mW C^{-1})**	**Thermal conductivity (W C^{-1} m^{-1})**	Metal Sphere radius (mm)	**Melting Slope (mW C^{-1})**	**Thermal conductivity (W C^{-1} m^{-1})**	
PANI	0.75	0.70	0.089	0.69	0.58	0.084	**0.25*** [K.Catterjee et al. (2013)],
PANI/ Bi$_2$Te$_3$	0.72	0.74	0.093	0.74	0.74	0.094	**0.11*** [K. Catterjee et al. (2013)]
Bi$_2$Te$_3$	0.73	1.49	0.161	0.75	0.84	0.108	**0.15*** [K.Catterjee et al. (2013)], **1.25** [E. Ashalley et al. (2015)]

*Room temperature measured values

Figure (7): The Slopes of the DSC melting peaks for the experiments for In with/ without the powders: A) 0 KGy and B) 50 KGy.

Although the irradiation process, the melting peak's area differences and slight deviations in the melting slopes for the samples the thermal conductivities of PANI and PANI/ Bi_2Te_3 do not affect strongly but in case of Bi_2Te_3 decreased more with irradiation process that confirmed from the structural characterization. The slight decrease in thermal conductivity of the PANI and PANI/Bi_2Te_3 was predicted due to the influence of radiation on the vibrational and rotational motion of the PANI chains by reducing them because the Gamma irradiation makes the chains more rigid. But there are a lot of parameters could affect the reduced values of thermal conductivities of the samples such as i) Heat lost in different ways like convection and radiation; ii) the thermal resistances are not equal for all samples; iii) the change of thermal conductivity with temperature which it might not distribute uniformly on the surfaces of the samples; iv) the slight change in the dimensions of the samples that could affect the thermal conductivity calculations; v) the weights of the samples influence their thermal conductivities; vi) thermal gradients between the reference metal and the samples could not be perfect [**K. Chatterjee et al. (2013), E. Ashalley (2015)**]. It should be noted that the effect due to Gamma-irradiation on the shape and the area of the melting peak of (In) that we will deal with in the future works.

Conclusion:

Nano-Structured compositions were achieved by solvothermal method. The irradiation process in case of PANI and PANI/ Bi_2Te_3 was lowering the unit cell volume while the grain size was increased for both of them. The thermal conductivity does not affect strongly from the irradiation but due to the doping PANI with Bi_2Te_3 the thermal conductivity was higher than the

pure PANI. The most affected sample from 50 KGy irradiation dose was Bi_2Te_3 which appeared on lowering the peak intensities, the grain size, the unit cell volume and thermal conductivity measurements.
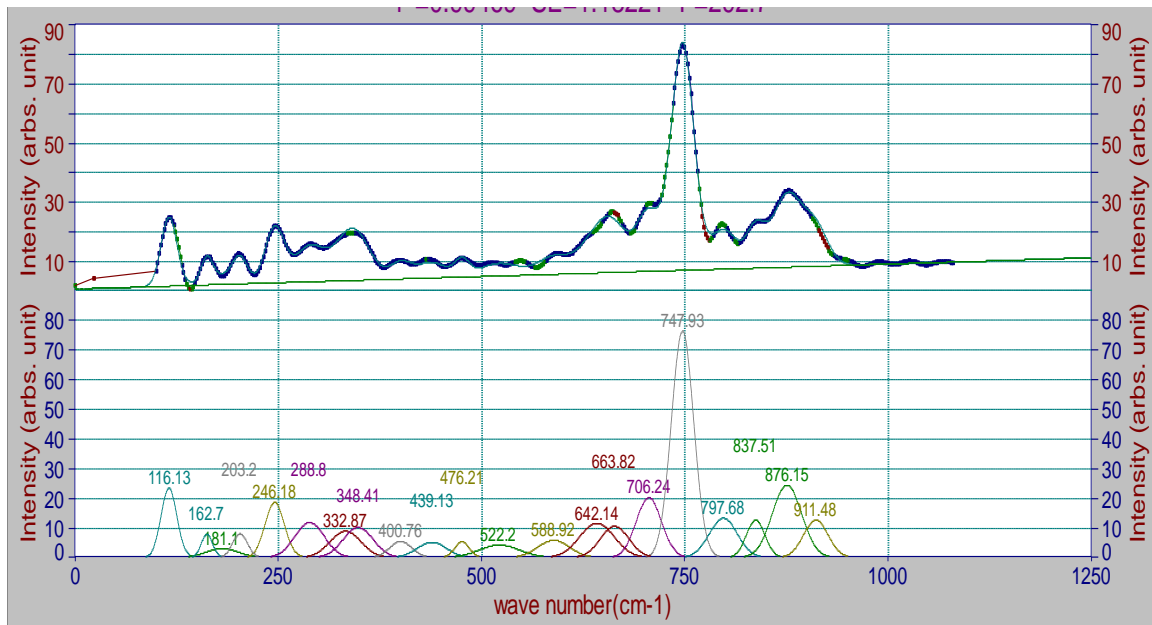
Appendix:

Figure (1): Fitted Raman spectrum pattern for irradiated 50 KGy Bi_2Te_3 sample

with 50*50 mm^2 laser spot size
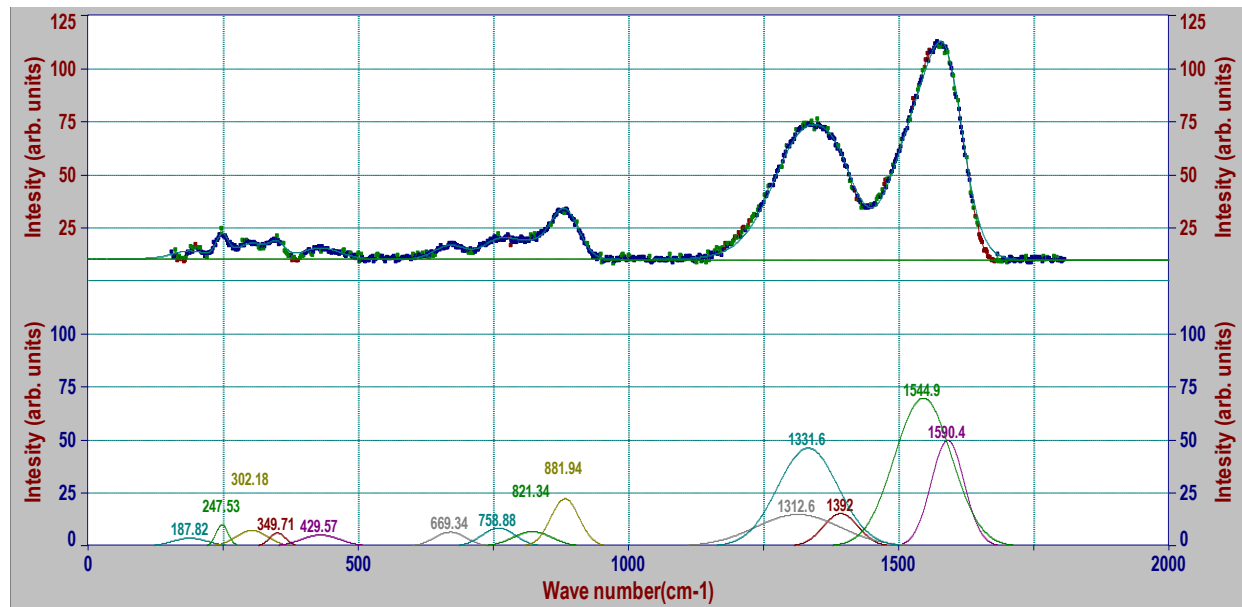

Figure (2): Fitted Raman spectrum pattern for PANI with 50*50 mm^2 laser spot size
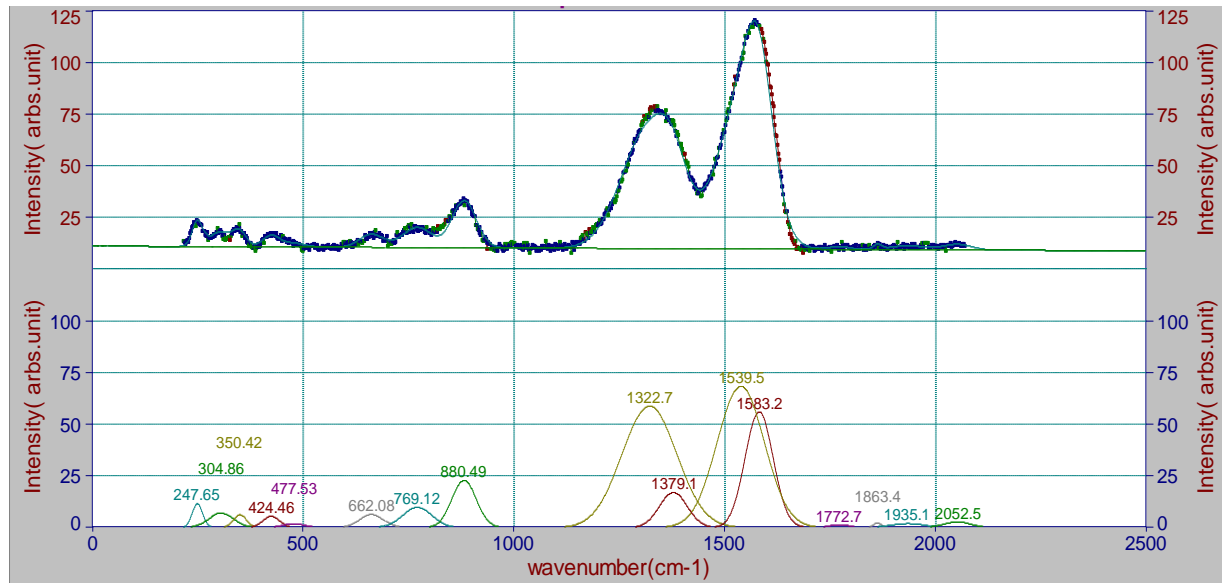
353

Figure (3): Fitted Raman spectrum pattern for irradiated 50 KGy PANI/Bi_2Te_3

with 50*50 mm^2 laser spot size.

References:

A. Shakouri, S. Li "Thermoelectric Power Factor for Electrically Conductive Polymers", IEEE, (1999), 2000, 402–406.

C.P. Camirand, "Measurement of thermal conductivity by differential scanning calorimetry", Thermochim. Acta.417 (2004) 1–4.

D.Sa´nchez-Rodrı´guez D.,J.P. Lo´pez-Olmedo, J. Farjas, P. Roura, "Determination of thermal conductivity of powders in different atmospheres by differential scanning calorimetry", J. Therm Anal Calorim. (2015) 121, 469–73.

E. Ashalley, H. Chen, X. Tong, H. Li, Z. M. Wang, "Bismuth telluride nanostructures: preparation, thermoelectric properties and topological insulating effect", Front. Mater. Sci., (2015) 9,103.

H. Yan,N. Toshima "Thermoelectric properties of alternatively layered films of polyaniline and (+/-)-10-camphorsulfonic acid-doped polyaniline", Chem. Lett., (1999) 1217–1218.

G. Min, D. M. Rowe "Cooling performance of integrated thermoelectric microcooler" Solid-State Electron. (1999) 43, 923–9

G.J. Snyder , E.S. Toberer "Complex thermoelectric materials" Nature Mater. (2008) 7, 105–14

G. D. Keskar, R. Podila, L. Zhang, A. M. Rao, and L.D. Pfefferle" Synthesis and Raman Spectroscopy of Multipahsic Nanostructured Bi-Ti Networks with Tailored composition" , J. Phys. Chem. C 117 (2013) 9446−9455

G. Louarn, M. Lapkowski, S. Quillard, A. Pron, J.P. Buisson, S. Lefrant" Raman Spectroscopic Studies of Regioregular Poly(3 alklthiophenes", J. Phys. Chem. 100(1996), 6998.

H. Mamur, M.R.A. Bhuiyan, F. Korkmaz, N. Mustafa, "A review on bismuth telluride (Bi$_2$Te$_3$) nanostructure for thermoelectric applications", J. Ren. and Sustain. Energy Rev., (2018) 82, 4159-4169.

 H. Xu, Y. Song, Q. Gong, W. Pan, X. Wu and S. Wang, "Raman Spectroscopy of epitaxial topological insulator Bi2Te3thin films" Modern Physics Letters B 29(15) (2015) 1550075 (10 pages).

I. Stark, M. Stordeur M., " New Micro Termoelectric Devices Based On Bismuth Telluride-Type Tin" Solid Films, 18th Int. Conf. on Thermoelectrics (Baltimore, MD) ,(1999) 465–72

J.H. Flynn, D.M. Levin, " A method for the determination of thermal conductivity of sheet materials by differential scanning calorimetry (DSC)" Thermochim. Acta. (1988)126 ,93–100.

J. P.Pouget, M. E. Jdzefowiczt ,A. J. Epstein, X. Tang,A. G.MacDiarmid" X-ray structure of polyanilin" Macromolecules 24, (1991) 779-789.

J. Tsukamoto,A. Takahashi,K. Kawasaki,"Structure and Electrical Properties of Polyacetylene Yielding a Conductivity of 10^5 S/cm", Japanese J. of Appl Phys Volume, 29(1990) , Issue 1, 125–30.

K. Chatterjee,A. Suresh,S. Ganguly, K. Kargupta, D. Banerjee "Bismuth nitrate doped polyaniline–Characterization and properties for thermoelectric application" Mater. Charact., 60, (2009)   597–601.

K. Chatterjee, M. Mitra, K. Kargupta, S. Ganguly, D. Banerjee "Synthesis, characterization and enhanced thermoelectric performance of structurally ordered cable-like novel polyaniline–bismuth telluride nanocomposite", Nanotechnology, (2013)   24, 215703 .

L. Wang, Q. Yao, H. Bi, F. Huang, Q. Wang and L. Chen" PANI/graphene nanocomposite films with high thermoelectric properties by enhanced molecular ordering", J. Mater. Chem. A 3 (2015), 7086–7092

M. Pujula, D. Sa´nchez-Rodrı´guez, J. Pere Lopez-Olmedo, J. Farjas, P. Roura, "Measuring thermal conductivity of powders with differential scanning calorimetry" J. Therm Anal Calorim, (2016) 125 ,571–577.

M. Cochet, G. Louarn, S. Quillard, J.P. Buisson, S. Lefrant" theoretical and experimental vibrational study of emeraldine in salt form", J. Raman Spectrosc. 31(2000), 1041

M. Tagowska, B. Palys, K. Jackowska"Polyaniline nanotubes annion effect on confirmation and Oxidation state of Polyaniline studied by Raman spectroscopy" Synth. Met. 142(2004), 223

M. A. Carvalho Mazzeu, L. K. Faria, A. de Moura Cardoso, A. M. Gama, M. R. Baldan, E. S. Gonçalves "Structural and Morphological Characteristics of Polyaniline Synthesized in Pilot Scale" J. Aerosp. Technol. Manag., São José dos Campos. 9 (2017), 39-47

N. Mateeva, H. Niculescu, J. Schlenoff, L.R. Testardi "Correlation of Seebeck coefficient and electric conductivity in polyaniline and polypyrrole" J. of Appl. Phys, (1998) 83(6), 3111–7.

N. Toshima, M. Imai,S. Ichikawa, (2011) Organic–Inorganic Nanohybrids as Novel Thermoelectric Materials: Hybrids of Polyaniline and Bismuth(III) Telluride Nanoparticles, J. Electron. Mater., 40, 898–902.

N. S. Abishek,K. Gopalakrishnan, K. Naik "Influence of gamma ray irradiation on stoichiometry of hydrothermally synthesized bismuth telluride nanoparticles" , AIP Conference Proceedings, (2018), 1953, 030067

S.R. Hostler,P. Kaul, K. Day, V. Qu, C. Cullen,A. R. Abramson "Thermal and electrical characterization of nanocomposites for thermoelectric IEEE ITHERM (2006) 24, 07803295,1400–5.

S. Bhadra,D. Khastgir "Determination of crystal structure of Polyaniline and substituted Polyaniline through powder X-ray diffraction analysis", Polymer Testing, 27, (2008) 851–857.

T.M. Tritt "Holey and Unholey Semiconductors", Science, (1999) 283, 804–5

T.M. Tritt, B. H. Öttner, L. D. Chen "Thermoelectrics: Direct Solar Thermal Energy Conversion", MRS Bull., (2008) 33, 366–7

V. Russo, A. Bailini, M. Zamboni, M. Passoni, C. Conti, C.S. Casari, A. LiBassi, C.E. Bottani" Raman Spectroscopy of Bi-Te thin films", J. Raman Spectrosc. 39 (2008) 205.

X. Xu, L.Chen, C.Wang, Q.Yao, C.Feng "Template synthesis of hetero structured polyaniline/Bi_2Te_3 nanowires", J., Solid State Chem., (2005) 178, 2163-6.

X.Zhao, B. S. Hu, H.M. Zhao, J. T. Zhu " thermoelectric properties of $Bi_{0.5}Sb_{1.5}Te_3$/polyaniline hybrids prepared by mechanical blending**,** J. Mater. Lett. (2002) 52147–9.

Y. Hiroshige, M. Ookawa, N. Toshima "High thermoelectric performance of poly(2,5-dimethoxyphenylenevinylene and its derivatives Synthetic ", Metals, (2006) 156, 1341–7.

Z.H. Zheng, P. Fan, T.B. Chen, Z.K. Cai, P.J. Liu, G.X. Liang, D.P. Zhang, X.M. Cai "Optimization in fabricating bithmuth thin films by ion beam sputtering deposition Thin Solid Films 520 (2012) 5245–5248

الملخص باللغة العربية

التأثير الاشعاعى على كل من التوصيلية الحرارية للمركبات النانومترية من PANI/ Bi₂Te₃

مصطفي سعيد أحمـد شلبى¹ ، نشوى محمد محمود يوسف¹ ، حمدية عبدالحميـد زايـد²
هــانى محمـد هاشـــم ³، لبنى علـى عبدالوهـاب¹

١- مركزبحوث و تكنولوجيا الاشعاع- الطاقة الذرية
٢- قسم الفيزياء-كلية البنات –جامعة عين شمس
٣- قسم الفيزياء-كلية العلوم- جامــــــعة حلوان

البحث يحتوى على دراسة خاصة بالمركبات النانومترية المشععة بأشعة جاما عند KGy ٥٠ لكل من البولى أنيلين (PANI) وBi₂Te₃, PANI/ Bi₂Te₃ وذلك من خلال عملية التحضير بطريقه المحاليل المعرضة للتسخين عند درجات حرارة منخفضة تصل الي ١٠٠ مئوية. التركيب البنائي و الخواص التركيبية للمركبات تم دراستها باستخدام حيود الاشعة السينية. التوصيلية الحرارية قيست باستخدام جهاز التحليل الحرارى (DSC) وقد وجد ان عينة Bi₂Te₃ قد تأثرت قيمة التوصلية الحرارية لها قبل وبعد التشعيع أكثر وهذا ما يتفق مع ما تم تعيينه سابقا من خلال حيود الاشعه السينيه. في حين ظهور تاثيرات ضعيفة على قيم التوصيلية الحرارية لمركبى (PANI) و PANI/ Bi₂Te₃ قبل وبعد عملية التشعيع من خلال اشعة جاما لذلك للطبيعة البوليمرية بهذه المركبات.